PACS numbers: 81.05.Uw; 65.40.–b; 42.25.Hz
DOI: 10.1070/QE2002v032n04ABEH002200

Measurement of thermal conductivity of polycrystalline CVD diamond by laser-induced transient grating technique

E.V.Ivakin, A.V.Sukhodolov, V.G.Ralchenko, A.V.Vlasov, A.V.Khomich

***Abstract*. The tangential thermal diffusivity $D_{\|}$ and thermal conductivity $k_{\|}$ of diamond plates grown from the gaseous phase by chemical vapour deposition (CVD diamond) are determined by the transient grating technique in the temperature range 25 – 200 °C. Samples of insulating and boron-doped polycrystalline diamond of thickness about 0.3 mm and diameter 63 mm were synthesised in a microwave discharge in mixtures of methane and hydrogen. In view of the intense light scattering by the samples, a photosensitive grating recording technique was developed and used for measurements. It was found that the value $k_{\|}$ amounts to 18 – 20 W cm^{-1} K^{-1} at room temperature, approaching the thermal conductivity of the highest purity single crystals of diamond. A comparison of the value of $k_{\|}$ with the normal thermal conductivity $k_{\perp}$ determined by the flash method reveals a thermal conductivity anisotropy of about 10 % – 20 % associated with the texture of the diamond film, the normal component of thermal conductivity being larger than the tangential component. Boron-doped diamond displays a dependence of the transient grating kinetics on the excitation wavelength. The obtained results indicate that CVD diamond is a promising material for preparing efficient heat sinks, especially of large size, used in microelectronic devices and laser engineering.**

Keywords: *polycrystalline diamond, semiconducting diamond, thermal conductivity, thermal diffusivity, transient grating technique*.

1. Introduction

Recent advances in the technique of synthesis of diamond from the gaseous phase (chemical vapour deposition, or CVD) have made it possible to prepare polycrystalline diamond in the form of plates having an area of tens of square centimetres and a thickness exceeding 1 mm. Many physical parameters of CVD diamond are close to those of the best single crystals found in nature [1, 2]. Promising applications of CVD diamond include the fabrication of heat sinks for semiconductor lasers, microwave transistors and multichip modules [3], optical elements for high-power CO_2 lasers [4, 5], UV detectors [6], windows for powerful gyrotrons and klystrons [2, 7].

The high thermal conductivity of diamond plays a significant role in many applications. The best single crystals of natural diamond of the IIa type have the highest thermal conductivity $k = 20 - 24$ W cm^{-1} K^{-1} at room temperature among other materials. Depending on the synthesis conditions, the thermal conductivity of polycrystalline diamond plates may vary over a wide range. Hence, it is quite important to control the heat transport parameters, preferably by contactless and quick methods. Generally speaking, polycrystalline CVD diamond is thermally inhomogeneous over its thickness (because the size of crystallites increases gradually in the growing layer), and also anisotropic (because the grains grow in the form of columns oriented along the normal to the surface). As a rule, the normal thermal diffusivity $D_{\perp}$ and thermal conductivity $k_{\perp}$ are larger than the tangential thermal diffusivity $D_{\|}$ and thermal conductivity $k_{\|}$ (along the plate). The thermal conductivity anisotropy may be as high as 50 % [8].

In view of these circumstances, the heat transfer was studied by using well-known methods, which provide information about the heat transfer in directions parallel and perpendicular to the sample surface. These methods are the transient grating (TG) technique and the flash method [9 – 11].

The TG technique is based on the creation of a transient thermal grating in the sample using interfering laser beams. First measurements of the thermal diffusivity of diamond by this technique were made in 1988 [12, 13] using a transient grating excited at 10.6 μm. Although other versions like the beam-deflection method [14] and the radiation technique [15, 16] are now available for reading out gratings, the method of diffraction probing by a cw laser [17, 18] remains the most suitable for solving the problem of temperature profile control in the excitation region.

The thermal diffusivity $D_{\|}$ along the sample surface can be determined from the measured time τ_d of exponential relaxation of the diffraction for a thermal grating having the period Λ using the relation $D_{\|} = \Lambda^2/(8\pi^2\tau_d)$ [17]. Numerous theoretical investigations have shown that this relation is valid in many situations of practical importance, including the problem under study. An advantage of the TG technique

E.V.Ivakin, A.V.Sukhodolov B.I.Stepanov Institute of Physics, National Academy of Sciences of Belarus, prosp. F.Scoryny 70, 220072 Minsk, Belarus; e-mail: ivakin@ifanbel.bas-net.by;
V.G.Ralchenko, A.V.Vlasov Natural Sciences Center, General Physics Institute, Russian Academy of Sciences, ul. Vavilova 38, 119991 Moscow, Russia; e-mail: ralchenko@nsc.gpi.ru; savl@nsc.gpi.ru;
A.V.Khomich Institute of Radioengineering and Electronics, Russian Academy of Sciences, pl. akad. Vvedenskogo 1, 141190 Fryazino, Moscow oblast, Russia; e-mail: perov@ms.ire.rssi.ru

Received 8 February 2002
Kvantovaya Elektronika **32** (4) 367 – 372 (2002)
Translated by Ram Wadhwa

is that it is possible in principle to 'feel' the layers of the material at various depths from the surface by varying the grating period because the characteristic penetration depth for heat in an isotropic medium is $\sim \Lambda/\pi$ [14]. However, a depth profile of the tangential thermal diffusivity can be obtained only in the case of surface absorption of the laser energy.

The flash method is based on the measurement of the propagation time of a laser-induced thermal wave from one side of the film to the opposite side. This gives the value of normal thermal diffusivity $D_\perp$, which is basically averaged over the sample thickness.

In this work, we used the TG technique and the flash method for measuring the thermal diffusivity and the thermal conductivity in two orthogonal directions for two types of high-purity CVD diamonds: the insulating and semiconducting boron-doped diamonds.

2. Experimental

Diamond plates were grown at the Natural Sciences Centre, General Physics Institute, Russian Academy of Sciences, on silicon substrates of diameter 63 mm in a microwave discharge using a reaction mixture of methane and hydrogen [19]. Sample A (No. 112) of thickness 0.33 mm was synthesised under the following conditions: methane concentration was 2 %, pressure in the chamber was 100 Torr, and microwave power was 5 kW at a frequency of 2.45 GHz. This material is transparent, its resistivity at room temperature being about 10^{14} Ω cm. Sample B (No. 125) of thickness 0.38 mm was doped with boron in the course of synthesis [20]. The resistivity of this blue semiconducting diamond is 10^3 Ω cm. The Raman spectra of both samples contain only a narrow line (of width about 3 cm^{-1}) of diamond at 1332 cm^{-1}, and do not reveal any other phases. Rectangular plates of size 5×5 and 6×8 mm were cut by a laser beam from the initial discs removed from the substrate, and were polished mechanically until the surface roughness was below 10 nm.

The optical absorption of plates was determined from the transmission spectra T_{IR} measured with double-beam Specord M400 and M80 spectrophotometers in the spectral ranges 0.18 – 0.9 μm and 2.5 – 50 μm, respectively. The effective absorption coefficient α^* was assumed to be equal to $(1/h)\ln(T_{IR}^0/T_{IR})$, where h is the thickness of the diamond film and T_{IR}^0 is the transmission calculated for the purest natural diamond of type IIa. According to the data of spectral ellipsometry (measurements were made by V.I.Kovalev at the Institute of Radioengineering and Electronics, Russian Academy of Sciences), the refractive index of the investigated samples differs by no more than 0.01 from that of natural diamond.

The experimental setup for the measurement of $D_\parallel$ or $k_\parallel$ by the transient grating technique is shown in Fig. 1. The gratings were induced by a single-pulse LF114 Nd : YAG laser with a DKDP crystal harmonic generator. The pulse repetition rate and the duration of the generated pulses were 10 Hz and 9 ns, respectively. The pulse energy in the sample plane was 1 – 3 mJ for the wavelengths 1064 and 266 nm.

A relief diffraction grating beamsplitter was used to form two interfering beams. Up to 80 % of the energy was pumped to minus and plus first orders, whereas the zeroth order was absent. The beamsplitter was imaged with a reduction on the sample using a confocal system, the two

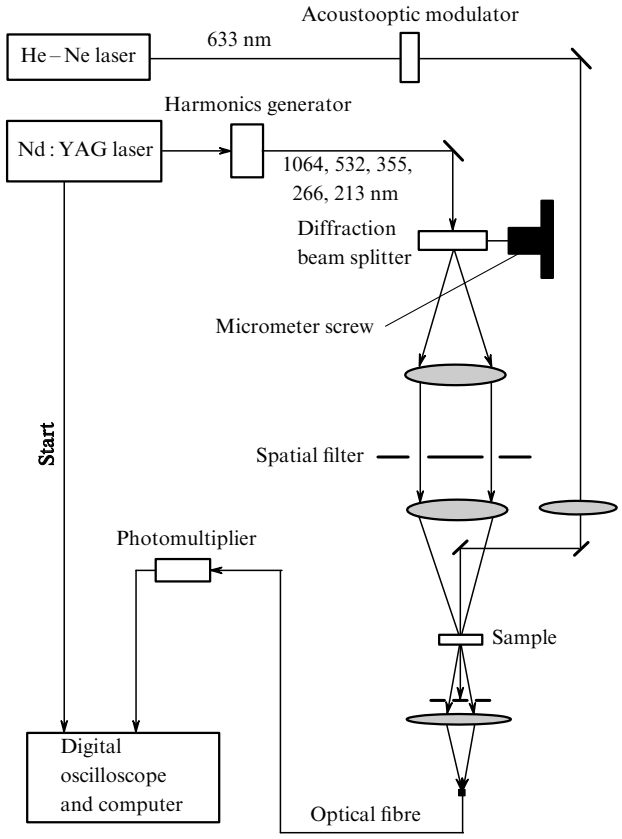

Figure 1. Experimental setup for measuring the tangential thermal diffusivity by the TG technique.

symmetric beams formed in the process being subjected to spatial filtration. The TG period can be varied stepwise in the interval 30 – 120 μm by changing beamsplitters.

The TG excitation region was probed by a cw He – Ne laser. The spatially filtered optical diffraction signal coupled to an optical fibre was incident on a photomultiplier and then fed to a digital oscilloscope for data storing and processing. The use of an acoustooptic Q switch, synchronised with the pulsed laser operation, in the probing beam reduces the current through the photomultiplier caused by light scattering, thereby preserving sensitivity and linearity. The sample holder is equipped with a heater and a temperature control system.

The setup has certain peculiar features, which make it possible to obtain reliable data for real samples containing macroscopic and microscopic inhomogeneities. The optical imperfection of samples usually leads to an uncontrollable deflection and scattering of the probe beam, and hence to a considerable distortion of the results of measurements. The first peculiarity of the setup shown in Fig. 1 is that two diffraction orders are recorded photometrically instead of one, as is usually the case with other setups. We described earlier [18, 21] the two-aperture method of compensating the effect of macroinhomogeneities of the samples. Using this principle, we can reduce the error in the measurement of the lifetime τ of the thermal grating from random error to systematic error, which can be taken into account easily in an analysis of the results of measurements.

The second peculiarity is associated with the phase-sensitive recording of the thermal grating to reduce the

effect of light scattering on the results of measurement of τ. It was mentioned in the earliest publications on TGs [22] that the mixing of coherent background with the diffraction signal on a photosensitive detector can be used to enhance the diffraction signal by controlling the phase of the diffracted beam through heterodyning. However, this useful property becomes a nuisance in the course of precise measurements because of the random nature of the coherent scattering background. Indeed, the one-exponential attenuation of the temperature wave in the sample in the simplest case leads to a two-exponential attenuation of the diffraction signal $I_d(t)$ with decay constants differing by a factor of two [23]:

$$I_d(t) = I_b + I_d(0)\exp\left(-\frac{2t}{\tau}\right) + 2\gamma[I_b I_d(0)]^{1/2}\exp\left(-\frac{t}{\tau}\right)\cos\varphi\,.$$

Here, $\tau = \Lambda^2/4\pi^2 D$ is the quantity being measured; $I_d(0)$ is the intensity of the diffracted beam for $t = 0$; I_b is the coherent background intensity; φ is the random phase difference between the diffraction field and the field of scattering at the detector surface; and γ is the coherence of the mixing fields.

In the scheme shown in Fig. 1, we suggest the principle of eliminating the third component in the above relation, which is based on the recording of two arrays of accumulated realisations separated by a half-period thermal grating shift accomplished by a transverse displacement of the diffraction beamsplitter by a quarter period. Subsequent summation of these arrays automatically eliminates the second (slower) exponential term, thus reducing the error in the course of fitting of results.

To demonstrate the efficiency of the proposed method, we carried out model measurements of $D_\parallel$ in a glass plate of thickness 100 μm. We first performed measurements for a sample of an optical quality, and then one of its surfaces was frosted slightly, which resulted in the appearance of background scattering. Circles in Fig. 2 show the diffraction kinetics for the initial sample of optical quality. As expected, the kinetics is described by a single exponential curve with constant $\tau = 65.5$ μs, corresponding to a thermal diffusivity $D_\parallel = 5.15 \times 10^{-3}$ cm^2 s^{-1}.

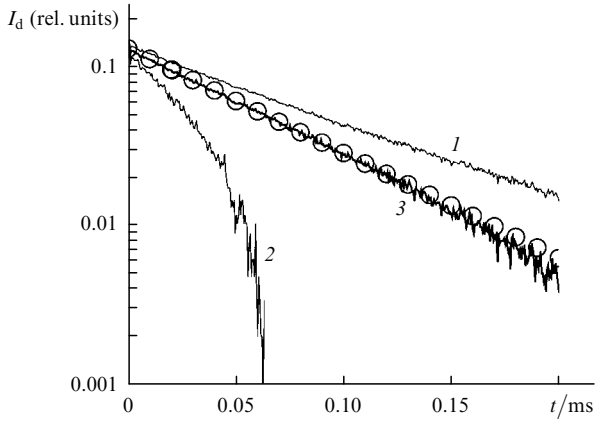

Figure 2. Time dependences of the diffraction intensity I_d for a glass plate of thickness 100 μm: circles correspond to the initial optical-quality sample; curves (*1*) and (*2*) correspond to a ground plate for two TG positions shifted by half-period; curve (*3*) is the sum of curves (*1*) and (*2*) for the thermal grating period $\Lambda = 51.6$ μm and an excitation wavelength of 266 nm.

A different type of diffraction pattern was observed in the case of the scattering plate. The first accumulation of 100 realisations led to curve (*1*) in Fig. 2. After the first accumulation, the interference pattern at the sample was displaced by a half-period, and a second array of 100 realisations was detected as shown by curve (*2*), which differs significantly from curve (*1*). Finally, the summation of both arrays led to curve (*3*), which passes almost entirely through the points corresponding to the sample of optical quality. The mean square deviation of the measured $D_\parallel$ from $D_\parallel$ for the sample of optical quality was ±3 %. The lowering of the influence of scattering is especially important in polycrystalline diamond where scattering occurs from internal grain boundaries.

The thermal diffusivity $D_\perp$ in the direction normal to the sample surface was measured at room temperature by the pulsed radiation thermometry (flash method) [10, 24]. A pulsed 1.06-μm, 8-ns Nd : YAG laser excites on the sample surface a thermal wave, which passes through the sample. The propagation time of the thermal wave to the opposite side of the sample is determined from the time dependence of the IR radiation intensity measured at the back of the sample by an HgCdTe detector with a time resolution of 300 ns. A metal waveguide is placed between the sample and the detector to ensure the maximum collection of thermal radiation. The absorption at the surface of the transparent sample is provided by depositing a thin layer of Ti on the illuminated side of the sample. A similar layer is deposited on the opposite side of the sample to increase the yield of thermal radiation. The variation in the sample temperature in the course of measurements is insignificant, being only 1–3 °C, and hence the thermal data obtained can be treated as room-temperature data.

3. Discussion of results

3.1 Optical properties

The IR transmission spectra T_{IR} and absorption spectra α^* in the visible region are shown for samples A and B in Fig. 3. The fundamental absorption edge in diamond lies in the UV region at 0.225 μm. The two-phonon fundamental lattice absorption band lies at 5 μm (2000 cm^{-1}). The absorption of light in sample A in the visible region is due to single nitrogen impurity atoms occupying the substitution sites in the diamond lattice. The concentration of paramagnetic nitrogen in sample A determined from the UV absorption spectra by the method [25] was 3×10^{17} cm^{-3}. Paramagnetic nitrogen at such low concentrations does not affect the thermal conductivity directly [26], but may induce structural defects in diamond grown from the gaseous phase [25], which exert a more significant effect on heat transport. Note that along with impurities and defects, scattering of light at the surface and in the bulk of the diamond film makes an additional contribution to the absorption spectra. The concentration of the impurity bound hydrogen, measured from the intensity of the C–H vibrational absorption band in the region of 3.33–3.57 μm (2800–3000 cm^{-1}) is about 6×10^{18} cm^{-3}. The concentration of hydrogen may serve as a qualitative indicator of the defect structure of diamond because hydrogen is assumed to decorate these defects [11, 25].

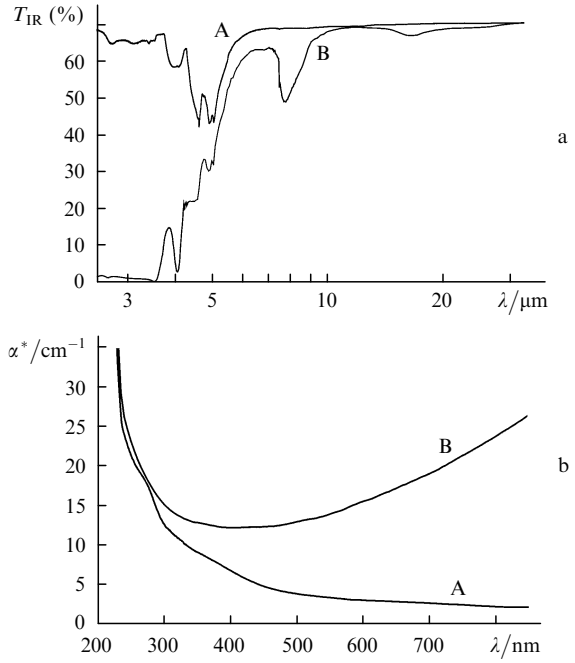

Figure 3. (a) IR transmission spectra and (b) UV–visible absorption spectra for diamond samples A and B.

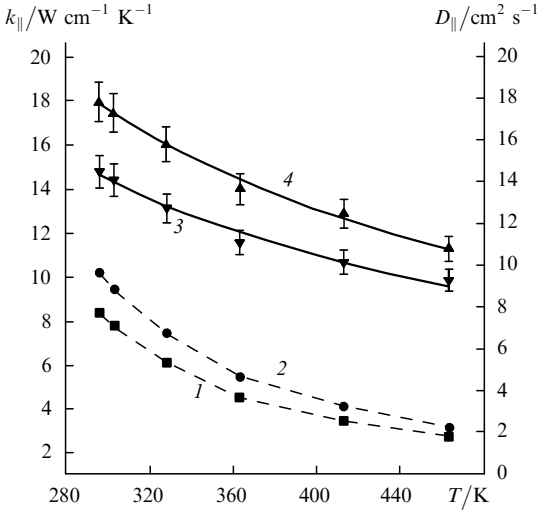

Figure 4. Temperature dependences of the thermal diffusivity $D_\parallel$ (curves *1*, *2*) and thermal conductivity $k_\parallel$ (curves *3*, *4*) of samples A (curves *1*, *3*) and B (curves *2*, *4*) of CVD diamonds. The solid curves correspond to the approximation by the power function $k \sim T^{-n}$.

In accordance with the generally accepted classification of diamonds, the boron-doped sample B is a type IIb diamond possessing semiconducting properties due to the presence of the acceptor impurity. The lattice absorption region for type IIb diamonds is characterised by absorption bands with maxima at 4.07 μm (2460 cm^{-1}), 3.56 μm (2810 cm^{-1}), and 3.41 μm (2936 cm^{-1}) (Fig. 3a). In addition, a band at 7.75 μm (1290 cm^{-1}) is also observed in the region of one-phonon transitions, which belongs to an uncompensated boron acceptor impurity in the sample. The absorption related to the acceptor transitions between the ground state and the excited states of the boron acceptor impurity is superimposed on two- and three-phonon absorption in the crystal lattice, and a continuous structureless absorption associated with the photoionisation of the acceptors is observed above 0.37 eV (3.35 μm). The short-wavelength part of this absorption extends to the visible spectral region and imparts a typical blue colour to boron-doped diamonds (see Fig. 3b). The concentration of the uncompensated acceptors determined from the IR spectra using the known relations [27] between the intensities of the characteristic absorption bands is equal to 6×10^{17} cm^{-3}.

3.2 Tangential thermal conductivity

The temperature dependences of the thermal diffusivity $D_\parallel$ and thermal conductivity $k_\parallel$ of CVD diamonds obtained by the TG technique are presented in Fig. 4. The following measurement parameters were used: the lattice period $\Lambda = 78.5$ μm and the excitation wavelength $\lambda = 266$ nm for sample A, and $\Lambda = 131$ μm, and $\lambda = 1064$ nm for sample B. At room temperature, $D_\parallel = 8.4$ and 10.1 cm^2 s^{-1} for samples A and B, respectively, and the values of these parameters decrease by a factor of more than three upon an increase in temperature to 200 °C. The fluctuations of $D_\parallel$ over the sample area did not exceed 10 % – 15 %. In view of the smallness of the optical absorption in samples at the excitation wavelengths, thermal gratings were produced almost uniformly over the sample thickness, so that the obtained values of $D_\parallel$ can be treated as averaged over the thickness of the sample.

Thermal conductivity was determined from the relation $k_\parallel = D_\parallel \rho C$, where $\rho = 3.515$ g cm^{-3} and C are the density and specific heat of diamond, respectively. Because of the high Debye temperature of diamond $\Theta = 1860$ K, the specific heat strongly varies in the temperature interval considered above, by about 100 %. The data on the temperature dependence $C(T)$ were taken from studies [26, 28] of diamond single crystals, because the density and specific heat for CVD diamond coincide [29] within an error of 1 % with the corresponding values for natural single crystals. At room temperature, the value of thermal conductivity is $k_\parallel = 14.5$ and 17.8 W cm^{-1} K^{-1} for samples A and B, respectively.

Only scant data on thermal conductivity at temperatures above room temperature are available for natural semiconducting diamonds, which are encountered very rarely. A set of 18 samples of blue natural single crystals of diamond was studied in Ref. [30]. The thermal conductivity of these diamonds belonging to type IIb did not differ much from the nitrogen-free samples of the IIa type, and was 18.4 – 20.2 W cm^{-1} K^{-1} at temperature $T = 320$ K, and 11.4 – 13.5 W cm^{-1} K^{-1} at $T = 450$ K. The decrease in thermal conductivity upon heating is due to an increase in the frequency of phonon–phonon collisions [26, 31], and a dependence $k \sim T^{-1}$ (the temperature is in kelvins) should be expected [31] at very high temperatures of the order of Θ, when this scattering mechanism dominates. By approximating the experimental curves (*3*) and (*4*) in Fig. 4 by a power function $k \sim T^{-n}$, we found that $n = 0.95 \pm 0.07$ (sample A) and 1.03 ± 0.05 (sample B) in the investigated temperature range. These values of n are in accord with the measurements made by Burgemeister [30] who found that $n \approx 1.26$ for crystals of IIa type in the interval 320–450 K, while the value of n decreases down to ~ 0.6 for diamonds with a lower thermal conductivity. Note that for CVD diamonds with a high degree of imperfection ($k \sim 5$ W cm^{-1} K^{-1}), the thermal conductivity almost does not change in the temperature range from 293 to 393 K [29].

3.3 Normal thermal conductivity

The values of $D_\perp$ and $k_\perp$ measured by the flash method were found to be higher by 20 % and 12 % than the corresponding values of $D_\parallel$ and $k_\parallel$ for samples A and B, respectively (Table 1). An anisotropy of the order of 10 % – 20 % is quite typical of polycrystalline diamond films [8, 15, 29], which is due to their columnar structure and also because the impurities and defects are concentrated predominantly near the grain boundaries. Since the local thermal conductivity increases with distance from the lower fine-grain side of the film (in contact with the substrate) [32], we can assume that the local coefficients $k_\perp$ exceed 20 W cm^{-1} K^{-1} in the upper coarse-grain layer, at least in sample B. Thus, the thermal properties of boron-doped CVD diamonds are close to those of natural semiconducting single crystals. To our knowledge, measurements of thermal diffusivity and thermal conductivity of CVD diamonds of this type were made for the first time.

Table 1. Resistivity ρ_0, tangential and normal thermal diffusivities $D_\parallel$ and $D_\perp$, and thermal conductivities $k_\parallel$ and $k_\perp$ of diamond samples A and B.

Sample	ρ_0/ Ω cm	$D_\parallel$/ cm^2 s^{-1}	$D_\perp$/ cm^2 s^{-1}	$k_\parallel$/ W cm^{-1} K^{-1}	$k_\perp$/ W cm^{-1} K^{-1}
A	10^{14}	8.4	9.8	14.5	17.4
B	10^3	10.1	11.2	17.8	20.0

3.4 Nonthermal refraction in boron-doped diamond

A comparison of the excitation of transient gratings by IR (curve *1*) and UV (curve *2*) radiation reveals interesting peculiarities in the diffraction kinetics of boron-doped samples (Fig. 5). Curve (*2*) has two components, a fast one associated with the formation of thermal grating, and a slow one associated apparently with the presence of boron (this spectral effect is not observed in undoped samples). Note that the components correspond to induced refractive indices of opposite signs. This is indicated by going through zero of the diffraction intensity 0.3 μs after the beginning of the process. At this instant, the components make identical contributions to diffraction (zero on the intensity scale corresponds to the background scattering). An analogous pattern was observed earlier for synthetic diamond single crystals [33], although the above-mentioned components have the same sign in that case.

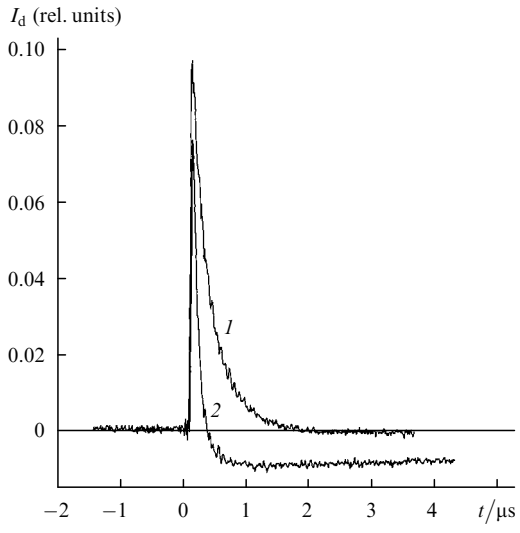

Figure 5. Diffraction intensity kinetics for the semiconducting sample B for TG excitation at 1064 (curve *1*) and 266 nm (curve *2*); $\Lambda = 131$ (curve *1*) and 77 μm (curve *2*).

The slow diffraction kinetics shown in Fig. 5 was observed due to long-lived refraction induced in the film by UV radiation. IR radiation does not excite the higher levels related to boron, and hence the slow component is not observed. Further experimental studies are being undertaken at present to determine the origin of the observed long-lived refraction.

4. Conclusions

The temperature dependences of thermal diffusivity and thermal conductivity of insulating and boron-doped polycrystalline diamond synthesised in a microwave discharge were measured by the pulsed TG technique in the temperature range 25 – 200 °C. It was found that at room temperature, k attains the values 18 – 20 W cm^{-1} K^{-1}, approaching the thermal conductivity of perfect single crystals of diamond. A comparison with the data obtained by the flash technique reveals an anisotropy of about 10% – 20% in the thermal conductivity along ($k_\parallel$) and across ($k_\perp$) the film surface, associated with the texture of the diamond film, the normal component of thermal conductivity being larger than the tangential component. Long-lived refraction induced by pulsed UV radiation at the grating was observed in a semiconducting diamond. The advancement of the technology of synthesis of high-quality CVD diamonds makes this material promising for fabricating effective heat sinks and for use in microelectronic devices and laser engineering.

Acknowledgements. This research was supported by the Belarus State Committee on Science (Grant No. M-20-2001) and by the Russian Federation programme 'Leading Research Schools' (Grant No. 00-15-96559).

References

1. Coe S.E., Sussmann R.S. *Diamond Relat. Mater.*, **9**, 1726 (2000).
2. Ralchenko V.G., Konov V.I., Vlasov I.I. Leont'ev I.A. *Proceedings of the VII International Scientific and Technical Conference 'High Technologies in Russian Industry'* (Moscow, 2001) p. 246.
3. Eden R.C. *Diamond Relat. Mater.*, **2**, 1051 (1993).
4. Kononenko V.V., Konov V.I., Pimenov S.M., Prokhorov A.M., Pavel'ev V.S., Soifer V.A. *Kvantovaya Elektron.*, **26**, 9 (1999) [*Quantum Electron.*, **29**, 9 (1999)].
5. Brierley C.J., Beck C.M., Kennedy G.R., Metcalfe J., Wheatley D. *Diamond Relat. Mater.*, **8**, 1759 (1999).
6. Whitfield M.D., Lansley S.P., Gaudin O., McKeag R.D., Rivzi N., Jackman R.B. *Diamond Relat. Mater.*, **10**, 715 (2001).
7. Garin B.M., Kopnin A.N., Parshin V.V., Ralchenko V.G., Chigryai E.E., Konov V.I., Mazur A.B., Parkhomenko M.P. *Pis'ma Zh. Tekh. Fiz.*, **25**, 85 (1999).
8. Graebner J.E., Jin S., Kammlott G.W., Bacon B., Seibles L., Banholzer W. *J. Appl. Phys.*, **71**, 5353 (1992).
9. Graebner J.E. *Diamond Films and Technology*, **3**, 77 (1993).
10. Ralchenko V., Vlasov A., Vlasov I., Zubov B., Nikitin A., Khomich A. *Proc. SPIE Int. Soc. Opt. Eng.*, **3484**, 214 (1997).
11. Twitchen D.J., Pickles C.S.J., Coe S.E., Sussmann R.S., Hall C.E. *Diamond Relat. Mater.*, **10**, 731 (2001).
12. Gorbachev V.V., Durasov V.M., Zezin R.B., Ivakin E.V., Rubanov A.S., Tatyanina N.A. *Phys. Stat. Sol. (b)*, **150**, 901 (1988).

13. Gorbachev V.V., Durasov V.M., Zezin P.B., Ivakin E.V., Rubanov A.S. *Inzh. Fiz. Zh.*, **56**, 754 (1989).
14. Käding O.W., Skurk H., Maznev A.A., Matthias E. *Appl. Phys. A*, **61**, 253 (1995).
15. Graebner J.E. *Rev. Sci. Instrum.*, **66**, 3903 (1995).
16. Graebner J.E., Ralchenko V.G., Smolin A.A., Obraztsova E.D., Korotushenko K.G., Konov V.I. *Diamond Relat. Mater.*, **5**, 693 (1996).
17. Eichler H.J., Gunter P., Pohl D.W. *Laser-Induced Dynamic Gratings* (Berlin: Springer, 1986).
18. Ivakin E.V. *Opt. Zh.*, **67**, 27 (2000).
19. Ralchenko V.G., Smolin A.A., Konov V.I., Sergeichev K.F., Sychov I.A., Vlasov I.I., Migulin V.V., Voronina S.V., Khomich A.V. *Diamond Relat. Mater.*, **6**, 417 (1997).
20. Polyakov V.I., Rukovishnikov A.I., Rossukanyi N.M., Ralchenko V.G. *Diamond Relat. Mater.*, **10**, 593 (2001).
21. Ivakin E.V., Ben V.N., Lazaruk A.M. Patent RF No. 2010221 (1992).
22. Pohl D.W. *IBM J. Res. Develop.*, **23**, 604 (1979).
23. Nagasaka Y., et al. *Rev. Sci. Instrum.*, **59**, 1156 (1988).
24. Vlasov A., Ralchenko V., Gordeev S., Zakharov D., Vlasov I., Belobrov P. *Diamond Relat. Mater.*, **9**, 1104 (2000).
25. Nistor S.V., Stefan M., Ralchenko V., Khomich A., Schoemaker D. *J. Appl. Phys.*, **87**, 8741 (2000).
26. Nepsha V.I., in *Handbook of Industrial Diamonds and Diamond Films* (N.Y.: Marcel Dekker, 1997) p. 169.
27. Chrenko R.M. *Phys. Rev. B*, **7**, 4560 (1973).
28. Victor A.C. *J. Chem. Phys.*, **36**, 1903 (1962).
29. Graebner J.E. *Diamond Relat. Mater.*, **5**, 1366 (1966).
30. Burgemeister E.A. *Physica B*, **93**, 165 (1978).
31. Berman R., in *The Properties of Diamond* (London: Acad. Press, 1979) p. 3.
32. Graebner J.E., Jin S., Kammlott G.W., Herb J.A., Gardiner C.F. *Nature*, **359**, 401 (1992).
33. Filippov V.V., Ivakin E.V., Lapchuk N.M., Rubanov A.S., Firsov S.P. *Proc. SPIE Int. Soc. Opt. Eng.*, **4358**, 148 (2001).